Ionics
https://doi.org/10.1007/s11581-020-03498-5

ORIGINAL PAPER

Protonic EDLC cell based on chitosan (CS): methylcellulose (MC) solid polymer blend electrolytes

Shujahadeen B. Aziz[1,2] · M. H. Hamsan[3] · Ranjdar M. Abdullah[1] · Rebar T. Abdulwahid[1,4] · M. A. Brza[1,5] · Aeyub Shahab Marif[1] · M. F. Z. Kadir[6]

Received: 29 November 2019 / Revised: 4 February 2020 / Accepted: 10 February 2020

Abstract

In this work, preparation and application of solid polymer blend electrolytes (SPBEs) based on chitosan: methylcellulose (CS:MC) incorporated with various amounts of ammonium iodide (NH_4I) salt are described. Solution cast technique was adapted for the preparation of the SPBE films. Structural investigation and extent of interaction of the NH_4I salt with the CS:MC film surface were conducted through X-ray diffraction (XRD) and Fourier transform infrared (FTIR) spectroscopy measurements. Electrical DC conductivity of the prepared samples was studied by electrochemical impedance spectroscopy. It is confirmed through transference number (TNM) analysis that ions are the dominant charge carrier in the polymer electrolyte system, in which the ionic (t_{ion}) and electron (t_{el}) transference numbers were found to be 0.934 and 0.036, respectively. Through the use of linear sweep voltammetry (LSV), the CS:MC:NH_4I system is found to experience electrolyte degradation at 2.1 V. The polymer blend electrolyte sample with highest DC conductivity property was also used as separator in electrical double-layer capacitor (EDLC) cell. Two identical activated carbon electrodes were used to sandwich the electrolyte film. Cyclic voltammetry (CV) was used to show the capacitive behavior of the fabricated EDLC cell, in which no redox peaks were observed. The EDLC was examined for 100 cycles at current density of 0.2 mA/cm^2. The values of specific capacitance and equivalent series resistance were determined to be 1.76 F/g, and 650 to 1050 Ω, respectively.

Keywords Polymer blend electrolyte · Ammonium salt · XRD and FTIR study · Impedance spectroscopy · EDLC study

Introduction

So far, electrical energy has been obtained from several resources, including 42% coal, 21% natural gas, 15% hydro, 14% nuclear, 5% oil, and 3% renewable energy devices [1]. The natural gas production and oil are expected to be lowered over the next few decades [2]. However, the emission of CO_2, which mainly comes from energy production of using coal, has been shown to be the main factor of global warming [3].

The renewable energy limitation is intermittent as well as variable. In order to employ the energy sources as feasible generation of power, energy storage plays a significant role. They store the surplus energy so as to supply the electrical equipment as well as they act as a backup power supply for the maintaining of instantaneous power. Several energy storages have been used. Batteries, flywheels, and supercapacitors can produce energy storage for a variety of solution [4]. Batteries have intense maintenance in addition to replacement problems, and checking their charge state is not easy. Flywheels can be low-cost at superior levels of power; however, still

✉ Shujahadeen B. Aziz
shujaadeen78@yahoo.com; shujahadeenaziz@gmail.com

[1] Advanced Polymeric Materials Research Laboratory, Department of Physics, College of Science, University of Sulaimani, Qlyasan Street, Sulaymaniyah, Kurdistan Regional Government, Iraq

[2] College of Engineering, Komar University of Science and Technology, Sulaymaniyah, Kurdistan Regional Government 46001, Iraq

[3] Institute for Advanced Studies, University of Malaya, 50603 Kuala Lumpur, Malaysia

[4] Department of Physics, College of Education, University of Sulaimani, Old Campus, Kurdistan Regional Government, Sulaymaniyah 46001, Iraq

[5] Manufacturing and Materials Engineering Department, Faculty of Engineering, International Islamic University of Malaysia, 50603 Kuala Lumpur, Gombak, Malaysia

[6] Centre for Foundation Studies in Science, University of Malaya, 50603 Kuala Lumpur, Gombak, Malaysia

Published online: 15 February 2020

flywheels are physically big along with several protection and maintenance problems associated with their installation. Supercapacitor is able to offer a high performance and low-cost solution at reasonable levels of power, due to its benefits for instance high charge-discharge current ability; excessive efficiency and extensive temperature range [5–7]. Such a device is so called electrochemical capacitors or ultracapacitors, in which energy stored and also released. Several characteristics of such supercacitors (SCs) make them to be promising to a large extent, for instant, relatively fast charging time, high power density, excellent cyclability and facile of fabrication [8, 9]. Three main types of SCs are taken into considerations, which are electrical double-layer capacitors (EDLC), pseudocapacitors, and hybrid battery-supercapacitors. Among these, EDLC possess the simplest and cost-effective of fabrication [10]. Activated carbon (AC) is often used as the electrode, owing to possession of micro porosity. This feature provides large surface area, which is beneficial for ions to accumulation at the interfacial region. A relatively high surface area of 1879 to 3313 m^2/g was obtained for AC [11].

In the current work, appropriate solid polymer electrolyte (SPE) is used as the electrode separator in the EDLC cell. SPE is usually considered as a heart of the device. SPEs provide several benefits, including satisfactory flexibility, ease of handling and plausible thermal and electrical properties as well [12]. It is worth-mentioning that the biopolymer is considered as a strong alterative to non-biodegradable synthetic polymers, for example, chitosan (CS), methylcellulose (MC), starch, dextran, gum, and carrageenan. One of most impressive characteristic of biopolymers is electrochemical stability along with an easy film forming ability. In order to be used in electrochemical devices, such as batteries, capacitors and solar cells [13, 14], the aforementioned properties are found to be crucial. In a report, a MC-PVDF based lithium batteries; specific capacity 150 mAh/g for 40 cycles was documented by Xiao et al. [15]. Park et al. have studied dye-sensitized solar cell using xanthan gum, in which SPE with a relatively high efficiency (4.78%) is obtained [16]. Recently, many research groups focused on employing various biopolymers as electrolyte and studied its potential application in EDLC device. For instant, Hamsan et al. study the potato starch-methyl cellulose as a host for NH_4NO_3 charge carriers in EDLC electrolyte [17], and corn starch-based biopolymer as a separator for EDLC were studied by Teoh et al. [18]. Additionally, potential application of biopolymers with different salts in EDLC device and its properties were found as an interest subject for the researchers [19, 20].

In the present work, polymer blend methodology has been performed with salt incorporation to reach some unique characteristics that are impossible to be achieved when using single polymers. Blending of CS with MC is found to be promising blending process. Both elements are known to be loaded with oxygen containing functional groups, which can be exploited for ionic conduction. The sources of these two bimolecular species are natural, which are crustaceans and green plant for CS and MC, respectively [21, 22]. To date, ammonium salt is used as a potential alternative of strong inorganic acids, such as sulfuric acid (H_2SO_4) and phosphoric acid (H_3PO_4). The use of these acids in energy devices result in chemical degradation [23].

To enrich the biopolymer electrolyte with ions, ammonium iodide (NH_4I) is employed. Among ammonium salts, NH_4I has a lattice energy value of 605.3 kJ/mol, which is relatively low compared to that of other ammonium salts, for instance, NH_4Cl (698 kJ/mol) and NH_4Br (665 kJ/mol) [24]. In other words, it easily dissociates into ion, which contributes in building up of charge double-layer in the EDLC [25]. Thereby, for electrode separating in the EDLC, it is proper to use this relatively high conducting CS:MC:NH_4I.

Materials and methods

Materials

From Sigma-Adrich, methylcellulose (MC) (4000 cP) and chitosan (CS) (310,000–375,000 g/mol) were purchased. From HmbG chemicals, EMPLURA, and Timcal, ammonium iodide (NH_4I), N-Methyl-2-pyrrolidone (NMP), and carbon black were purchased, respectively. From magna value, polyvinylidene fluoride (PVdF) and activated carbon (RP20) were purchased.

Electrolyte preparation

In the preparation of CS:MC host polymer blend, separately, 0.7 g of CS and 0.3 g MC were dissolved in 40 mL of 1% acetic acid for 3 h at room temperature. The solutions were then mixed and stirred for another 2 h until a homogeneous blend mixture was obtained [26]. NH_4I with various concentrations of 10, 20, 30, and 40 wt% were added to the CS:MC mixture and the fabricated samples were coded as CSMC1, CSMC2, CSMC3, and CSMC4, respectively. The plastic Petri dishes were used to keep the solution and then left to dry at room temperature. For further dryness, the formed films were placed in a desiccator containing silica gel prior to characterizations. Table 1 shows the composition of the samples.

Table 1 Composition of the CS:MC blend electrolytes

Sample code	CS:MC (0.7:0.3) g	NH_4I (wt.%)	NH_4I (g)
CSMC1	1	10	0.1111
CSMC2	1	20	0.2500
CSMC3	1	30	0.4285
CSMC4	1	40	0.6666

Structural and impedance characterization

X-Ray Diffraction (XRD) patterns were attained by means of Empyrean X-ray diffractometer, (PANalytical, Netherland) with working potential and current of 40 KV and 40 mA, correspondingly. The films were illuminated with a monochromatic CuKα X-radiation beam with a wavelength of 1.5406 Å and the X-ray diffraction glancing angles (2θ) was in the range between 5° and 80° with a step size of 0.1°.

To examine the pure film and incorporated films with NH_4I salt, Fourier Transform Infrared (FTIR) spectrophotometer (Thermo Scientific, Nicolet iS10) was employed in the wavenumber region from 3900 to 800 cm^{-1} and having a resolution of 2 cm^{-1}.

The gaining of the films impedance spectra was accomplished by means of HIOKI 3531 Z Hi-tester in the frequency region between 50 Hz and 1000 kHz. The fabricated samples were cut into tiny discs with 2 cm in diameter and then located between two electrodes stainless steel (SS) underneath spring pressure. The cell was joined to a computer equipped with a software to compute real (Z') and imaginary (Z") parts of the spectra of the complex impedance (Z*).

Electrochemical characterization

Ionic (t_{ion}) and electronic (t_{el}) transference number measurement (TNM) were determined from cell polarization of a cell system of stainless steel SS | highest conducting SPBE | SS at 0.80 V working potential. This analysis was performed by using V&A Instrument DP3003 digital DC power supply at room temperature. The values of t_{ion} and t_{el} were calculated using the following equations:

$$t_{ion} = \frac{I_i - I_{ss}}{I_i} \quad (1)$$

$$t_{el} = 1 - t_{ion} \quad (2)$$

where, I_i and I_{ss} are current at initial and steady state, respectively.

From Fig. 1, one can see the TNM experiment setup.

To identify the potential window (electrochemical stability of the SPBE samples), linear sweep voltammetry (LSV) was carried out, where the potential was swept linearly through the SS | highest conducting SPE | SS at 10 mV/s using Digi-IVY DY2300. The cell arrangement for TNM and LSV was shown in Fig. 2.

Fabrication and characterization of the EDLC

Planetary ball miller was used to grind 3.25 g of activated carbon with 0.25 g of carbon black for 20 min. At the same time, 0.5 g of PVdF was stirred in 15 mL NMP for 2 h. In to PVdF-NMP solution, activated-carbon powder was poured

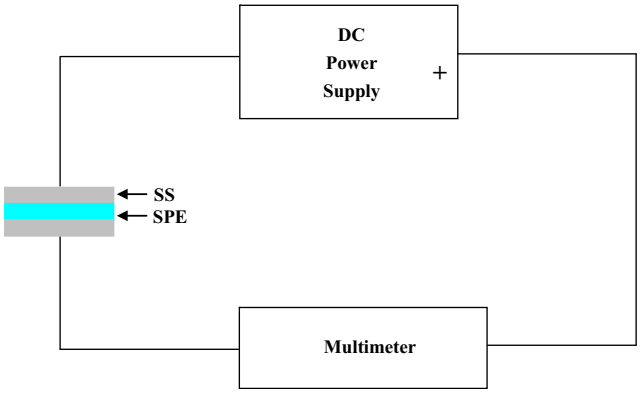

Fig. 1 Diagram of TNM experimental setup

and then stirred for 2 h until the appearance of thick black in color solution. An aluminum foil was pre-cleaned with acetone and then the prepared solution was poured on it. For aluminum foil coating process, a doctor blade was used. Afterwards, 2.01 cm^2 electrodes were dried in the oven at 60 °C and subsequently the dried electrodes were stored in desiccator with silica gel for further drying.

The final step was the arrangement of the fabricated EDLC as shown in Fig. 3. The cell was packed in a CR2032 coin cell like shape.

The fabricated EDLC was analyzed by using cyclic voltammetry (CV). For this purpose, a Digi-IVY DY2300 Potentiostat was used. The potential sweep was started from 0 to 0.9 V. The charge-discharge measurement was also carried out for the EDLC device, using Neware battery cycler (0.2 mA/cm^2). Both the specific capacitance (C_s) and equivalent series resistance (R_{esr}) were calculated using equations shown below:

$$C_s = \frac{i}{S_{dis} m} \quad (3)$$

$$R_{esr} = \frac{V_{drop}}{i} \quad (4)$$

where, the slope of discharge part (S_{dis}) was determined from charge-discharge plot and i and m are the applied current and activated carbon mass which were 0.4 mA and 81.2%, respectively. Eq. (3) was used to calculate the specific capacitance of the cell capacitor. A potential drop (V_{drop}) prior to discharging process was used to calculate the R_{esr}.

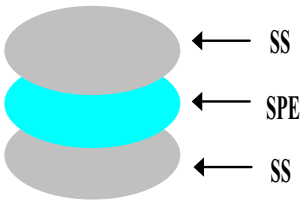

Fig. 2 Cell arrangement for TNM and LSV

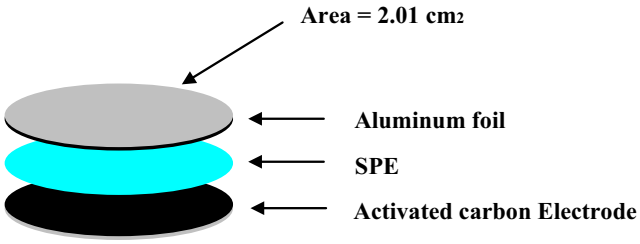

Fig. 3 Schematic illustration of the fabricated EDLC arrangement

Results and discussion

Structural study

XRD study

Figure 4*(a, b, and c)* shows the diffractograms of the pure CS and CS: MC films. It has been documented that the crystalline peaks for pure CS are recorded at 2θ = 15.1, 17.7 and 20.9° as a consequence of inter- and intra-hydrogen bonding between the functional groups of individual monomers and the chains [27, 28]. The semi-crystalline nature of MC is an inherent structural feature that enables X-ray examinations to be performed through the MC influences on the biopolymer matrix [29]. It has been reported that there exists only one hollow at 2θ = 19-21° for MC material, which originates from the intermolecular hydrogen bonding together with a short-distance order in the MC polymer chains [30–32]. An interesting point is that a broad peak at a diffraction angle 2θ (CuKα1,2) of 8.03° is recognized which is relate to the presence of trimethyl glucose repeating unit within the MC [29]. It can be seen that only one hump can be distinguished from the XRD pattern of CS:MC system [see Fig. 4(b)]. It can be verified from the broad humps that the CS:MC blend almost amorphous structure [33, 34]. Here, the idea of physical blending two or more polymers has been recognized to obtain a material with low crystallinity, allowing the conductivity to be enhanced. It is important to mention that polymer blends are mixtures of at least two structurally different polymers that joint together through secondary forces without forming any covalent bond [35, 36]. Figure 4 *(b,c)* shows the XRD pattern obtained for desired blend electrolyte samples. Interestingly, with addition of 20 wt.% of inorganic NH_4I salt into CS:MC matrix, the hollow intensity of the CS:MC was significantly lowered as can be seen in Fig. 4(b). This can be considered as an evidence of decreasing the crystalline region in the CS matrix [28]. It is obvious from Fig. 4(c) that addition of 40 wt.% of NH_4I salt to CS:MC mixture can result in more broadening of the hollow. Both peak broadening and lowering in intensity reveal that the amorphous region within the blended polymer body is a dominant. Another advantage of XRD analysis is that it can be used to anticipate the conductivity trend of the electrolytes [37]. The reason behind the lowering of crystallinity is due to the addition of the inorganic salt into the CS:MC system, is the complex formation between polar groups of the polymer and cations of the salt, owing to electrostatic interactions, and disrupting hydrogen bonding [28]. In accordance with the concept of Hodge et al.'s [38], there is a correlation between the peak intensity and the degree of crystallinity, in which the intensity change and broad nature of the XRD pattern are considered to be strong evidences of dominated amorphous behavior of the sample.

FTIR study

FTIR measurements were carried out to evidence the interactions that take place between the NH_4I salt and the CS:MC host polymers. Figure 5 *(a-c)* presents the FTIR spectra of CS:MC biopolymer electrolytes in the range of 800–3900 cm^{-1}. The peaks position shifting and changing in intensity of the bands have been considered as a proof of existence of whole organic functional groups in pure CS: MC and CS:MC:NH_4I electrolyte samples. Moreover, the existence of heteroatoms, e.g., O and N, in a desired fabricated polymer host as electrolyte was emphasized [29, 39]. A strong peak around 2900 cm^{-1} was observed and related to the C-H stretching modes as showed in Fig. 5b [40–42]. However, the intensity of that peak was lowered as the salt concentration increased. Another strong absorption band, between 1600 and 1700 cm^{-1}, was found to be attributed to the C = O stretching of the amide I vibration. The other modes that centered between 1480 and 1580 cm^{-1} were corresponded to the amide II vibration (C-N stretching and N-H bending) [43, 44]. It is seen that the main features of CS polymer are a single -NH_2 group and a couple of -OH groups in the repeating unit [45, 46]. A peak centered at 3359 cm^{-1} was indicated to be -OH stretching in the form of a broad peak, as shown in Fig. 5b**.** This has been significantly impacted by incorporation process as previously confirmed [40].

Based on previous works [32, 46], the characteristic FTIR spectra of MC and CS polymers have been shown by confirmation of the vibrational frequency peaks of -NH_2, O = C-NH, and – OH. Further confirmation is shown from Fig. 5b, where a shifting was occurred toward lower wave number in the bands of amino NH_2, O = C-NH and OH groups. This is a strong verification of interaction between the whole components of the polymer under study.

It is observable that the intensity of the peaks has decreased with noticeable peak position shifting as a consequence of the addition of NH_4I. Particularly, this emphasizes a strong interaction between the polymer body and amine salt through a coordination bond and eventually the complex formation [47, 48]. A peak around 1057 cm^{-1} was detected and associated to the C-O bond in ether as showed in Fig. 5a. Though, the intensity of that peak was shifted as the concentration of the NH_4I increased [31]. The oxygen atom in C-O-C ether

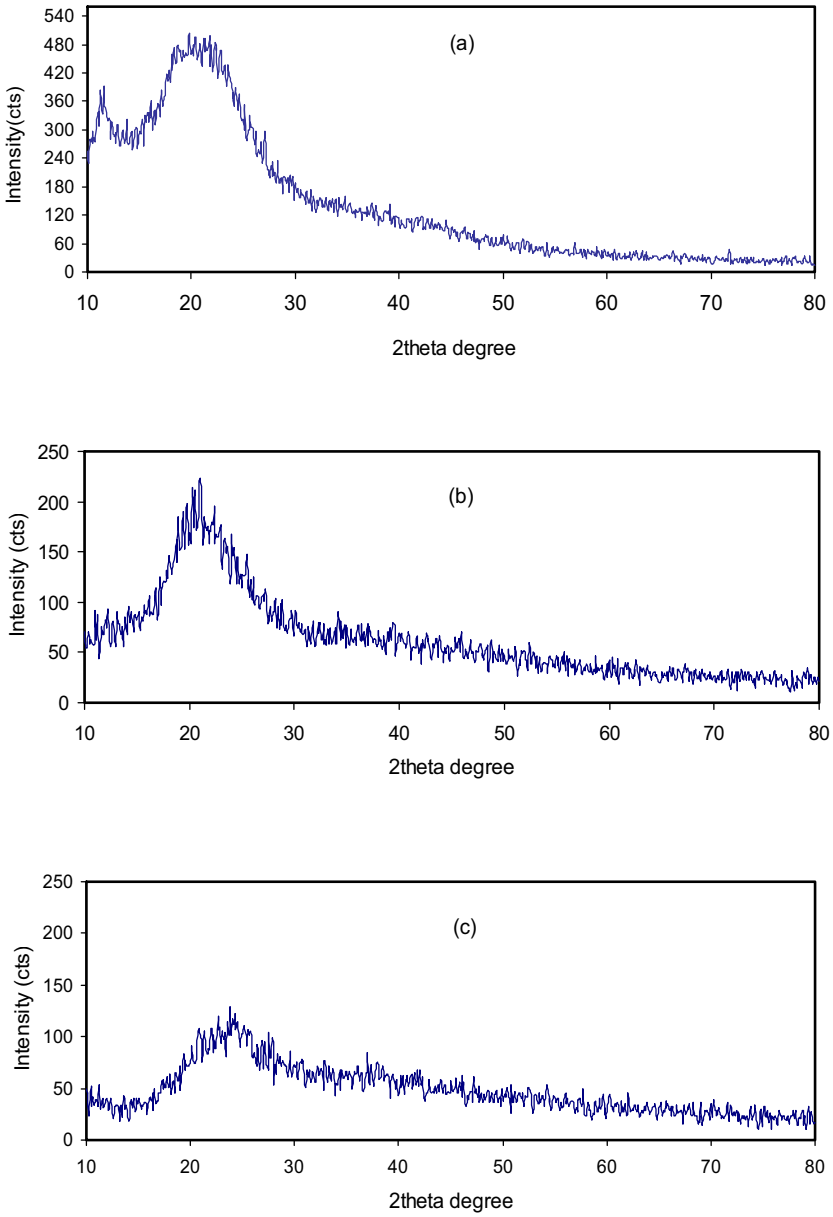

Fig. 4 XRD spectra of (a) pure CS, (b) CSMC2, and (c) CSMC4 electrolyte films

group in identical polymer is to produce polymer salt complexes through attracting the cation ions that provided by NH_4I [47]. In the present system, it is most obvious that NH^{4+} ion is coming from the NH_4I, in coordination with O atom of the ether group and the hydroxyl group in CS and MC host polymer blend. These interactions facilitate protonation in the desired electrolytes, where it is clearly verified as one looks at the shifting of hydroxyl group, C-O bond in ether, C = O and -NH_2 as shown in Fig. 5 ***(a-c)*** [31].

Impedance study

From the physics and chemistry perspectives, the study of ion transport mechanism in polymer electrolytes has been considered as one of the primary topics. In literature, researchers have carried out a massive effort in impedance analyses of solid polymer blend and nano-composite polymer electrolytes [49–52]. This technique has shown relative advantage over other techniques in studying electron and ion transport in polymer electrolytes and mixed conductor systems [34, 53–58]. In an early study [34], impedance spectroscopy (EIS) has been used successfully in determining the phase transition of PEO in CS based polymer electrolytes. In bulk materials, electrical charge displacements have been performed through two distinct physical phenomena; firstly, a polarization phenomenon, which occurs when the charge motion is strictly confined in a localized volume of the matter; secondly, a collective diffusion phenomenon, which is

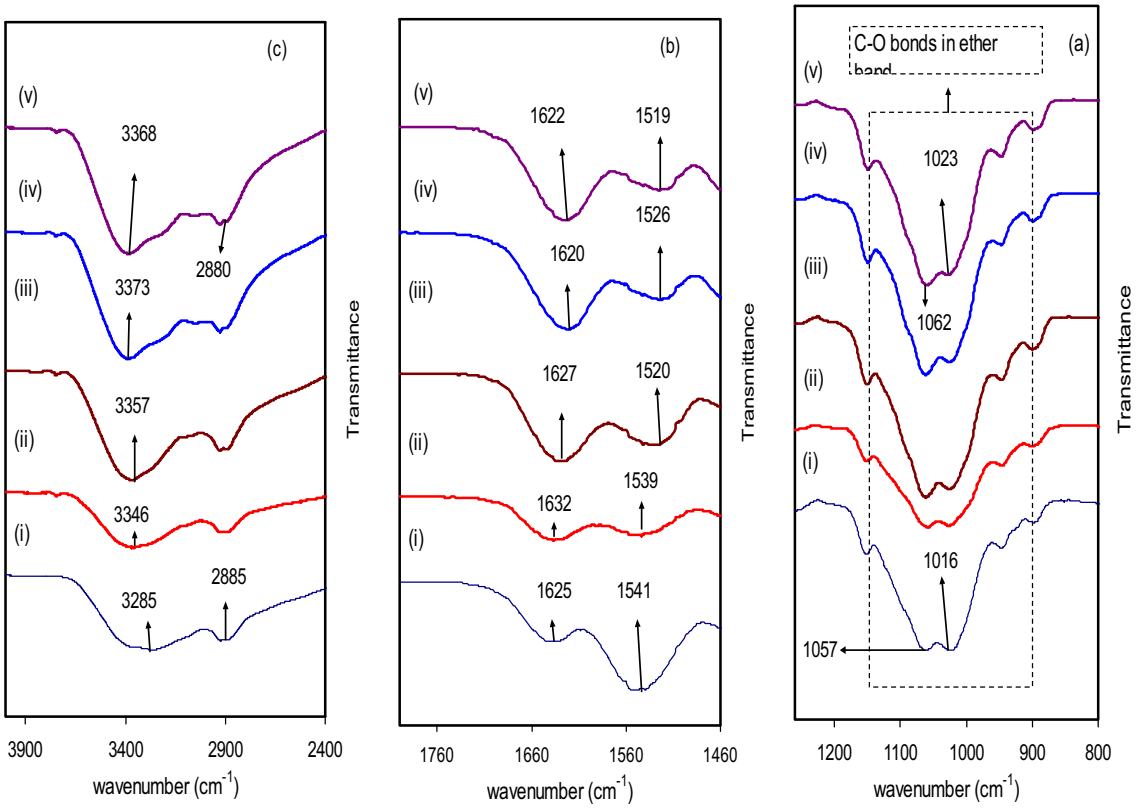

Fig. 5 FTIR spectra of (i) CS:MC (pure film), (ii) CSMC1, (iii) CSMC2, (iv) CSMC3, and (v) CSMC4 in the region (a) 800 to 1260 cm^{-1}, (b) 1460 cm^{-1} to 1760 cm^{-1}, and (c) 2400 cm^{-1} to 3900 cm^{-1}

responsible for the electrical charges to be displaced over long distances in materials. Subsequently, DC conductivity, σ_{dc}, has been then established [59]. For the AC conductivity, complex impedance spectroscopy, which relies on cell impedance/admittance measurements over a range of frequencies, has been used. In a comparison between the resistance and impedance, there is an account for phase difference. Clearly, for AC conductivity, the impedance (Z) has been used as opposition to the resistance, which can be calculated by addition of resistance to reactance [60]. Figure 6***(a-d)*** shows the impedance plots, i.e., the imaginary part (Z_i) as a function of real part (Z_r), of CS:MC:NH_4I complexes. From the results, a relatively high conductivity has been obtained. It is seen that with an increase in salt concentration, the bulk resistance decreases (see the insets of Fig. 6). It is noticeable from the figure that there is a domination of a pair of distinct regions, namely, the high- and low-frequency semicircle regions. They are due to the solid electrolyte's bulk influence and electrode polarization (EP, i.e., the effect of electrode blocking), respectively. This phenomenon is actually resulted from the emergence of electric double layer capacitances (EDLCs). The formation of EDLC is resulted from accumulation of charge at the solid electrode/electrolyte interfacial region [61]. The output EIS plot is composed of imaginary part versus the real part. It is confirmed that with an increase of salt concentration, there is a decrease in the bulk resistance, as shown in Fig. 6 (see the insets). From the impedance analysis, the bulk resistance (R_b) is determined from the point where semicircle intersects the real axis (Zr). For the determination of conductivity of the sample, one can apply the equation shown below based on both R_b and the sample dimensions:

$$\sigma_{dc} = \left(\frac{1}{R_b}\right) \times \left(\frac{t}{A}\right) \tag{5}$$

where, t and A are the thickness and surface area of the film, respectively. The calculated DC conductivities for all the samples are presented in Table 2. It is important to mention that one of the main requirements for applying EDLC is a blend electrolyte with a high DC conductivity.

Transference number analysis

In SPE system, the conduction process is indeed shown to be performed by both electron and ion. To determine the dominant charge carrier within a SPE system, it is appropriate to utilize the TNM technique. Figure 7 illustrates the effect of polarization of SPE system at a potential of 0.8 V. It can be seen from the figure that the initial current value is quite high

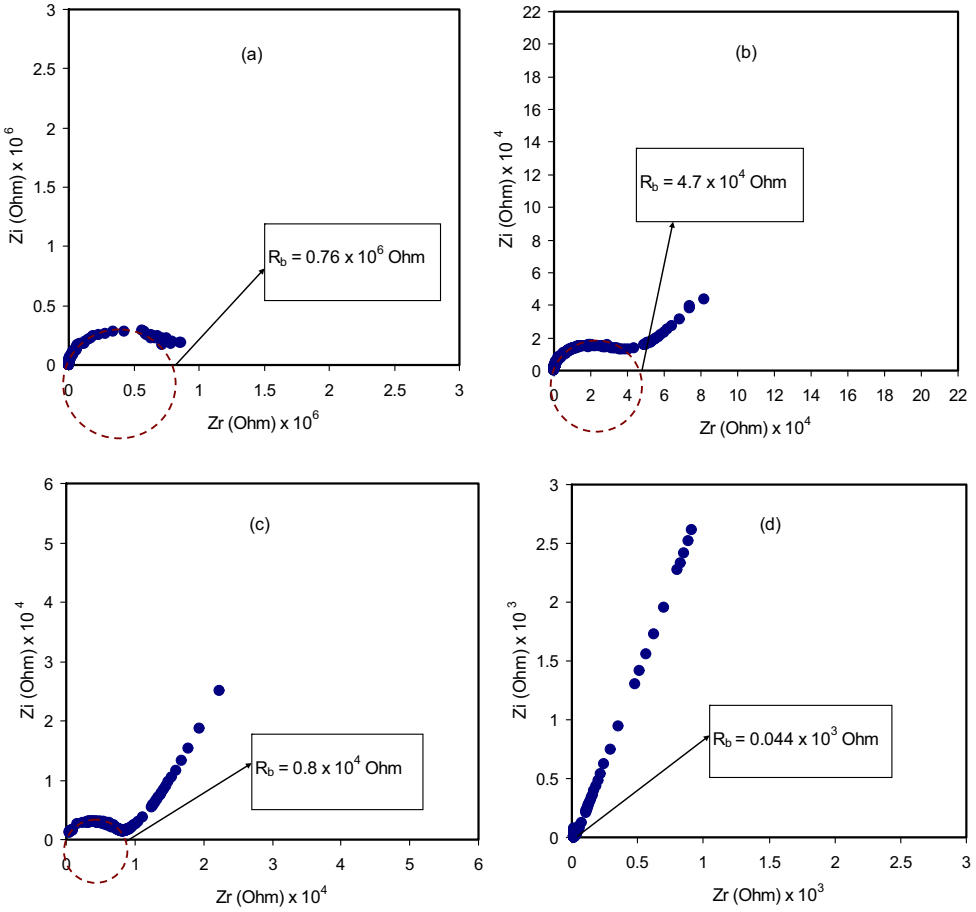

Fig. 6 Impedance plot for (a) CS:MC1, (b) CSMC2, (c) CSMC3, and (d) CSMC4

and found to be at 11.1 μA. This indicates that both electron and ion are contributing at the early stage of polarization process. At times beyond 20 s, the current become constant at 0.4 μA. This is found to be a characteristic of the stainless electrodes as a consequence of ionic blocking. This phenomenon is called steady-state, where electron can only make transitions from the SPE to the electrode phases. With the presence of electric field ions can be migrated toward the electrodes. This migration process is then balanced by diffusion due to the concentration gradient thus the cell is polarized. The polarization current is then exclusively carried by electrons [62].

The calculations of t_{ion} and t_{el} can be performed using Eqs. (1) and (2), respectively. It is observed that t_{ion} and t_{el} are relatively high and low with 0.934 and 0.036, respectively. This is the unique characteristic of an ionic conductor along with electron transfer [63, 64]. It is indicated from the value of t_{ion} that the charge carrier is entirely ion in the matrix of CS:MC. Here, the results in terms of these calculated parameters are found to be more satisfactory compared to those reported for NH_4I-based SPE systems. Samsi et al. [65] have documented that the value of t_{ion} is about 0.916 for a system consisting of both cellulose acetate (75 wt.%) and NH_4I

Table 2 Obtained DC conductivity of the CS:MC blend electrolyte samples

Prepared samples	DC Conductivity (S cm^{-1})
CSMC1	1.12×10^{-8}
CSMC2	1.8×10^{-7}
CSMC3	1.06×10^{-6}
CSMC4	1.93×10^{-4}

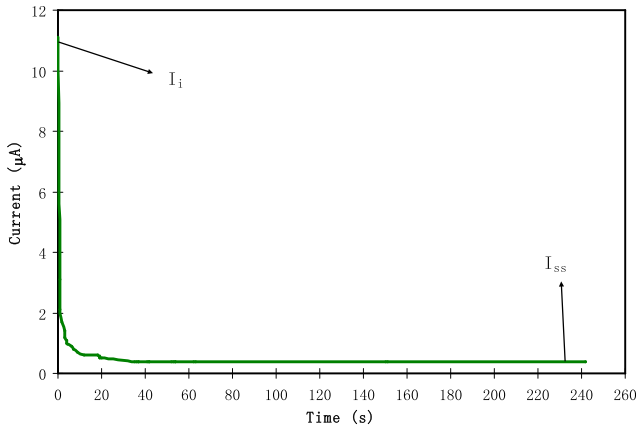

Fig. 7 Polarization of the highest conducting CS:MC:NH_4I system

(25 wt.%). The ionic contribution in poly (ethyl methacrylate)-NH_4I system with 60:40 ratio has been documented to be 0.85 [66]. Moreover, in another study, the t_{ion} has been recorded to be 0.905 for SPE of cellulose acetate-NH_4I incorporated with polycarbonate and zinc sulfate as plasticizer and filler [67].

Linear sweep voltammetry

Linear sweep voltammetry (LSV) is a powerful voltammetric technique where current at a working electrode can be measured while a potential is swept linearly with time across the working electrode and a reference electrode. From this technique, it is easy to decide whether the SPE is suitable for applications in electrochemical devices or not. Therefore, in this regards, it is shown to be very crucial technique. Figure 8 shows the LSV plot, where scan rate was 10 mV/s. It is shown that there is no noticeable change in the current as the potential increases. However, as the potential exceeds 2.1 V, the current has increased significantly, indicating decomposition potential of CS:MC:NH_4I system. From this result, it is verified that the SPE undergoes electrolyte degradation at the surface of SS electrode at the potential exceed the limit [68]. This kind of reaction exhibits instability of the SPE, which results in capacity fading and irreversible reaction as well [69]. Therefore, CS:MC:NH_4I system reaches one of the requirements to be used in protonic energy devices, where the minimum decomposition potential is required to be 1 V.

EDLC studies

Cyclic voltammetry

The capacitance of EDLC was usually examined from cyclic voltammetry. In the present work, the fabricated EDLC was tested at a scan rate of 50 mV/s in the potential window between 0 and 0.9 V. Figure 9 shows the CV plot of the EDLC

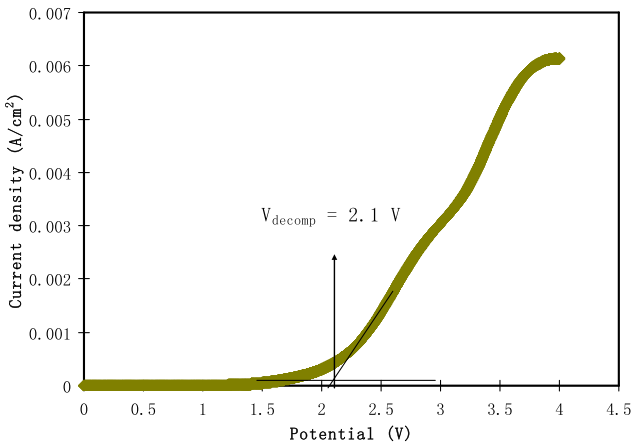

Fig. 8 LSV plot for the highest conducting CS:MC:NH_4I system at 10 mV/s

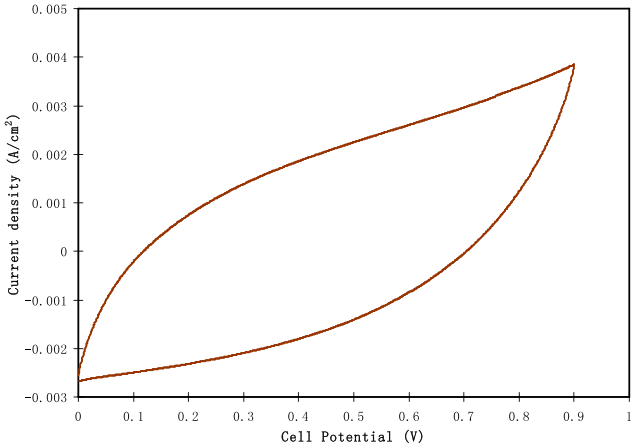

Fig. 9 The plot of cyclic voltammetry of the fabricated EDLC cell

device. One can see that there is no feature of redox peak in the CV profile, which indicates that cations and anions from NH_4I salt are absorbed at the surface of the carbonic electrodes rather than intercalation/deintercalation process [70]. This resulted in non-Faradaic reaction where ions form charge double–layer with electrons from the carbonic electrodes on the basis potential energy [71]. The shape of the CV is leaf-like shape rather than a perfect rectangular shape. However, the shape is satisfactory by taking into consideration of electrode roughness and internal resistance [72]. In comparison, the shape of CV in this work is quite similar to other biopolymer-based EDLC studies [73–75]. From Kant et al. point of view [76], cyclic voltammetry is an indicator of successful charge propagation.

Charge-discharge analysis

To examine the rechargeability of the EDLC, a 0.2 mA/cm^2 charge-discharge current rate was applied for 100 cycles, as shown in Fig. 10. In fact, as the current is applied, the charged ions start to migrate from the bulk region of the electrolyte to the opposite polarization electrodes, producing double layer charging. This is known as polarization or capacitive characteristic [77]. Figure 10 indicates this behavior; in which it can be evidenced through the discharge curve linearity. In order to

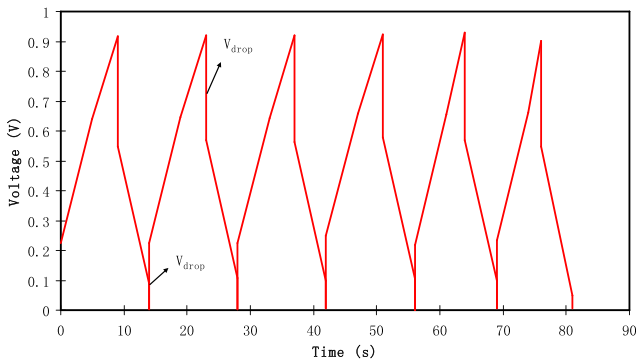

Fig. 10 Charge-discharge profile of the fabricated EDLC

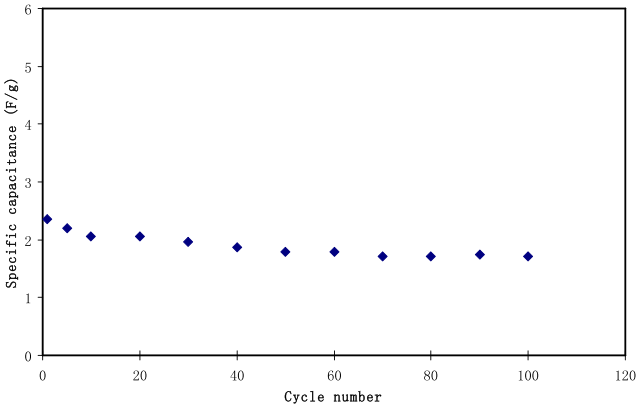

Fig. 11 Specific capacitance of the EDLC throughout 100 cycles

determine the specific capacitance (C_s) of the fabricated EDLC, Eq. 3 has been used. Figure 11 shows the obtained C_s values. At 1st cycle, the C_s was found to be 2.36 F/g and dropped to 1.95 F/g at 30th cycle. Such decrease of C_s can be attributed to the electrolyte-electrode contact imperfection [78]. An interesting observation has been achieved beyond 30th cycle, where C_s becomes constant with an average value of 1.76 F/g. When the sample material is positioned between the two electrodes, charge carriers transport within the polymer electrolyte film to create the EDLC. The electrolyte gradually becomes polarized and charges accumulate on both electrodes. This is apparently known as the ion polarization stabilization. Table 3 shows the value of C_s for other proton-based EDLC studies that documented in literatures. It is worthnoticing that the potential drops prior to the process of discharging commences as shown in Fig. 10. This provides an insight into the internal resistance of the fabricated EDLC, in which the R_{esr} can be calculated through Eq. 4. It is likely that the value of R_{esr} is situated within the range of 650–1050 Ω, as shown in Fig. 12. For the sake of comparison, the value is relatively high, which can be correlated to the presence of PVdF in the electrode composition. The insulator property of PVdF can block the electron migration in the

Table 3 Relative specific capacitance values of a number of proton-based EDLC systems

SPE system	C_s (F/g)	Cycles	Reference
Chitosan-H_3PO_4-Al_2SiO_5	0.22	100	[82]
Chitosan-H_3PO_4-NH_4NO_3-Al_2SiO_5	0.25	100	[82]
PVA-$NH_4C_2H_3O_2$	0.14	Not stated	[83]
MC-NH_4NO_3	1.67	100	[84]
PEO-LiTf-EMITf	1.70	Not stated	[85]
CS-MC-NH_4I	1.76	100	This work
Carboxymethyl cellulose (CMC)-NH_4NO_3	1.8	11	[86]
PEO-$Mg(Tf)_2$-EMITf	2.6–3.0	Not stated	[85]

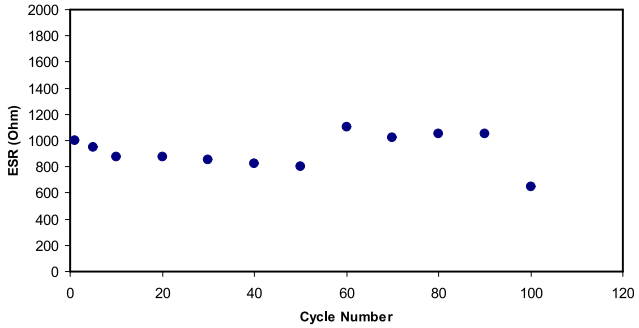

Fig. 12 Internal resistance of the EDLC throughout 100 cycles

carbonic electrons [79]. However, in the present work, the value of R_{esr} is still lower than other proton-based EDLC studies. [80, 81].

Conclusions

Solid polymer blend electrolytes (SPBEs) of chitosan (CS), methylcellulose (MC), NH_4I have been successfully prepared via solution cast technique. The structural analysis was successfully analyzed from the lowering intensity in the XRD. The peak position shifting occurred in the FTIR spectra confirmed a relatively strong interaction between the polymer blend components. The reduction in bulk resistance upon increasing salt concentration was proven through EIS analysis. The highest DC conductivity was found to be 1.93×10^{-4} S cm^{-1} for the CS:MC doped with 40 wt% of NH_4I. It was found that ions are dominant charge carrier, as t_{ion} was 0.934 while t_{el} was only 0.036. The relatively high electrochemical stability (2.1 V) of the biopolymer electrolyte was belonged to natural composition of the blend polymer. From CV profile of the fabricated EDLC no redox peaks were observed, showing the absence of undesired redox reaction at the surface of carbonic electrodes. The average specific capacitance was found to be 1.76 F/g with R_{esr} in the range of 650 to 1050 Ω. Ultimately, the relatively low value of specific capacitance was caused by the high value of equivalent series resistance.

Acknowledgments The authors gratefully acknowledge the financial support for this study from the Ministry of Higher Education and Scientific Research-Kurdish National Research Council (KNRC), Kurdistan Regional Government/Iraq. The financial support from the University of Sulaimani and Komar Research Center (KRC) and Komar University of Science and Technology are greatly appreciated.

Funding information This research was funded by the Ministry of Higher Education and Scientific Research-Kurdish National Research Council (KNRC), Kurdistan Regional Government/Iraq. The financial support from the University of Sulaimani and Komar Research Center (KRC) and Komar University of Science and Technology is greatly appreciated.

Compliance with ethical standards

Conflict of interest The authors declare no conflict of interest.

References

1. Yang Z, Zhang J, Kintner-Meyer MC, Lu X, Choi D, Lemmon JP, Liu J (2011) Electrochemical energy storage for green grid. Chem Rev 111:3577–3613
2. Powell CA, Morreale BD (2008) Materials Challenges in Advanced Coal Conversion Technologies. MRS Bull 33:309–315
3. Arunachalam, V. S.; Fleischer, E. L. The Global Energy Landscape and Materials Innovation MRS Bull 2008, 33, 264–288
4. Sibo Wang, Tongzhen Wei, Zhiping Qi. Supercapacitor Energy Storage Technology and its Application in Renewable Energy Power Generation System. Proceedings of ISES World Congress 2007 (Vol. I – Vol. V) pp 2805–2809
5. Schainker RB (2004) Executive Overview: EnergyStorage Options For A Sustainable Energy Future. Power Eng Soc Gen Meet 2: 2309–2314
6. Marin S. Halper, James C. Ellenbogen,"Supercapacitor: a brief overview", http://www.mitre.org. March 2006
7. Burke A (2000) Ultracapacitors: why, how, and where is the technology. J Power Sources 91:37–50
8. Zhi J, Yang C, Lin T, Cui H, Wang Z, Zhang H, Huang F (2016) Flexible all solid state Supercapacitor with high energy density employing black Titania nanoparticles as a conductive agent. Nanoscale 8:4054–4062
9. Andres B, Dahlstrom C, Blomquist N, Norgen M, Olin H (2018) Cellulose binders for electric double-layer capacitor electrodes: the influence of cellulose quality on electrical properties. Mat Des 141: 342–349
10. Yang I, Kim SG, Kwon SH, Lee JH, Kim MS, Jung JC (2016) Pore size-controlled carbon aerogels for EDLC electrodes in organic electrolytes. Curr Appl Phys 16(6):665–672
11. Hou B, Zhang T, Yan R, Li D, Mo Y, Yin L, Chen Y (2016) High specific surface area activated carbon with well balanced micro/ Mesoporosity for ultrahigh Supercapacitive performance. Int J Electrochem Sci 11:9007–9018
12. Yu J, Yan X, Ma Z, Mei P, Xiao W, You Q, Zhang Y (2018) Development of the PEO Based Solid Polymer Electrolytes for All-Solid State Lithium Ion Batteries. Polymers 10(11):1237
13. Nyuk CM, Isa MIN (2017) Solid biopolymer electrolytes based on carboxymethyl cellulose for use in coin cell proton batteries. J Sustain Sci Manag 2018:42–48
14. Woo HJ, Liew C, Majid SR, Arof AK (2014) Poly (ε-caprolactone)-based polymer electrolyte for electrical double-layer capacitors. High Perform Polym 26:637–640
15. Xiao SY, Yang YQ, Li MX, Wang FX, Chang Z, Wu YP, Liu X (2014) A composite membrane based on a biocompatible cellulose as a host of gel polymer electrolyte for lithium ion batteries. J Power Sources 270:53–58
16. Park SJ, Yoo K, Kim JY, Kim JY, Lee DK, Kim B, Kim H, Kim JH, Cho J, Ko MJ (2013) Water-based thixotropic polymer gel electrolyte for dye-sensitized solar cells. ACS Nano 7(5):4050–4056
17. Hamsan MH, Shukur MF, Kadir MFZ (2017) NH4NO3 as charge carrier contributor in glycerolized potato starch-methyl cellulose blend-based polymer electrolyte and the application in electrochemical double-layer capacitor. Ionics 23:3429–3453. https://doi.org/10.1007/s11581-017-2155-1
18. Teoh KH, Lim C, Liew C et al (2015) Electric double-layer capacitors with corn starch-based biopolymer electrolytes incorporating silica as filler. Ionics 21:2061–2068. https://doi.org/10.1007/s11581-014-1359-x
19. Kadir MFZ, Salleh NS, Hamsan MH, Aspanut Z, Majid NA, Shukur MF (2018) Biopolymeric electrolyte based on glycerolized methyl cellulose with NH4Br as proton source and potential application in EDLC. Ionics 24:1651–1662. https://doi.org/10.1007/s11581-017-2330-4
20. Tan HW, Ramesh S, Liew C (2019) Electrical, thermal, and structural studies on highly conducting additive-free biopolymer electrolytes for electric double-layer capacitor application. Ionics 25: 4861–4874. https://doi.org/10.1007/s11581-019-03017-1
21. Hariyawati NK, Saraswati LPA, Made Arcana I (2019) Properties of polymer electrolytes based on chitosan/poly(vinyl alcohol) for Lithium battery application. Am J Eng Res 8:135–143
22. Taghizadeh MT, Seifi-Aghjekohal P (2015) Sonocatalytic degradation of 2- hydroxyethyl cellulose in the presence of some nanoparticles. Ultrason Sonochem 26:265–272
23. Chartterjee B, Kulshrestha N, Gupta PN (2015) Electrical properties of starch-PVA biodegradable polymer blend. Phys Scr 90: 025805–025814
24. Jonson DA Some thermodynamic aspects of inorganic chemistry. Second edition, Cambridge University press 1982. Cambridge ISBN 0521242045
25. Buraidah MH, Arof AK (2011) Characterization of chitosan/PVA blended electrolyte doped with NH4I. J Non-Cryst Solids 357: 3261–3266
26. Aziz SB, Hamsan MH, Abdullah R, Kadir MFZ (2019) A Promising Polymer Blend Electrolytes Based on Chitosan: Methyl Cellulose for EDLC Application with High Specific Capacitance and Energy Density. Molecules 24:2503
27. Aziz SB, Abidin ZHZ, Kadir MFZ (2015) Innovative method to avoid the reduction of silver ions to silver nanoparticles in silver ion conducting based polymer electrolytes. Phys Scr 90:035808
28. Aziz SB, Kadir MFZ, Abidin ZHZ (2016) Structural, morphological and electrochemical impedance study of CS: LiTf based solid polymer electrolyte: Reformulated Arrhenius equation for ion transport study. Int J Electrochem Sci 11:9228–9244
29. Liebeck BM, Hidalgo N, Roth G, Popescu C, Böker A (2017) Synthesis and Characterization of Methyl Cellulose/Keratin Hydrolysate Composite Membranes. Polymers 9:91
30. Liu P, Xiangmei W, Zhong L (2013) Miscibility study of chitosan and methylcellulose blends. Adv Mater Res 750–752:802–805
31. Aziz NAN, Idris NK, Isa MIN (2010) Solid Polymer Electrolytes Based on Methylcellulose: FT-IR and Ionic Conductivity Studies. Int J Polym Anal Charact 15:319–327
32. Aziz S, Rasheed M, Ahmed H (2017) Synthesis of Polymer Nanocomposites Based on [Methyl Cellulose](1− x):(CuS) x (0.02 M≤ x≤ 0.08 M) with Desired Optical Band Gaps. Polymers 9(6):194
33. Aziz SB, Abidin ZHZ, Arof AK (2010) Effect of silver nanoparticles on the DC conductivity in chitosan–silver triflate polymer electrolyte. Physica B 405:4429–4433
34. Aziz SB, Abdullah RM (2018) Crystalline and amorphous phase identification from the tanδ relaxation peaks and impedance plots in polymer blend electrolytes based on [CS: AgNt] x: PEO (x-1)(10≤ x≤ 50). Electrochim Acta 285:30–46
35. Vanitha D, Bahadur SA, Nallamuthu N, Athimoolam S, Manikandan A (2017) Electrical Impedance Studies on Sodium Ion Conducting Composite Blend Polymer Electrolyte. J Inorg Organomet Polym 27:257
36. Aziz SB, Hamsan MH, Brza MA, Kadir MFZ, Abdulwahid RT, Ghareeb HO, Woo HJ (2019) Fabrication of energy storage EDLC device based on CS: PEO polymer blend electrolytes with high Li^+ ion transference number. Results in Physics 15:102584
37. Salleh NS, Aziz SB, Aspanut Z, Kadir MFZ (2016) Electrical impedance and conduction mechanism analysis of biopolymer

electrolytes based on methyl cellulose doped with ammonium iodide. Ionics 22:2157
38. Hodge RM, Edward GH, Simon GP (1996) Water absorption and states of water in semicrystalline poly(vinyl alcohol) films. Polym J 37:1371–1376
39. Lu G, Kong L, Sheng B, Wang G, Gong Y, Zhang X (2007) Degradation of covalently cross-linked carboxymethyl chitosan and its potential application for peripheral nerve regeneration. Eur Polym J 43:3807–3818
40. Aziz SB, Marif RB, Brza MA, Hassan AN, Ahmad HA, Faidhalla YA et al (2019) Structural, thermal, morphological and optical properties of PEO filled with biosynthesized Ag nanoparticles: new insights to band gap study. Results Phys 13:102220
41. Ramesh S, Yuen TF, Shen CJ (2008) Conductivity and FTIR studies on PEO-LiX [X: CF3SO3-, SO42-] polymer electrolytes. Spectrochim Acta - Part A Mol Biomol Spectrosc 69:670–675
42. Wen SJ, Richardson TJ, Ghantous DI, Striebel KA, Ross PN, Cairns EJ (1996) FTIR characterization of PEO + $LiN(CF_3SO_2)_2$ electrolytes. J Electroanal Chem 408:113–118
43. Idris A, Vijayaraghavan R, Rana UA, Fredericks D, Patti AF, MacFarlane DR (2013) Dissolution of featherkeratin in ionic liquids. Green Chem 15:525
44. Zhang Y, Zhao W, Yang R (2015) Steam flash explosion assisted dissolution of keratin from feathers. ACS Sustain Chem Eng 3: 2036–2042
45. Agrawal P, Strijkers GJ, Nicolay K (2010) Chitosan-based systems for molecular imaging. Adv Drug Deliv Rev 62:42–58
46. Aziz SB, Abidin ZHZ (2013) Electrical conduction mechanism in solid polymer electrolytes: new concepts to Arrhenius equation. J Soft Matter 2013:1–8
47. Nurhaziqah AMS, Afiqah IQ, Aziz MFHA, Aziz NAN, Hasiah S (2018) Optical, structural and electrical studies of biopolymer electrolytes based on methylcellulose doped with Ca(NO3)2. IOP Conf Ser Mater Sci Eng 440:012034
48. Sahli NB, Bin AAMM (2012) Effect of lithium triflate salt concentration in methyl cellulose-based solid polymer electrolytes. CHUSER 2012–2012 IEEE Colloq Humanit Sci Eng Res:739–742
49. Aziz SB, Karim WO, Brza MA, Abdulwahid RT, Saeed SR, Al-Zangana S, Kadir MFZ (2019) Ion transport study in CS: POZ based polymer membrane electrolytes using Trukhan model. Int J Mol Sci 20:5265
50. Aziz SB, Abdulwahid RT, Hamsan MH, Brza MA, Abdullah RM, Kadir MFZ, Muzakir SK (2019) Structural, impedance, and EDLC characteristics of proton conducting chitosan-based polymer blend electrolytes with high electrochemical stability. Molecules 24:3508
51. Sharma S, Dhiman N, Pathak D, Kumar R (2016) Effect of nanosize fumed silica on ionic conductivity of PVdF-HFP-based plasticized nano-composite polymer electrolytes. Ionics 22:1865–1872. https://doi.org/10.1007/s11581-016-1721-2
52. Sahu TB, Sahu M, Karan S, Mahipal YK, Sahu DK, Agrawal RC (2018) Study of electrical and electrochemical behavior on copper ion conducting nano-composite polymer electrolyte. Ionics 24: 2885–2892. https://doi.org/10.1007/s11581-017-2384-3
53. Aziz SB (2018) The mixed contribution of ionic and electronic carriers to conductivity in chitosan based solid electrolytes mediated by CuNt salt. J Inorg Organomet Polym 28:1942
54. Scrosati B, Croce F, Persi L (2000) Impedance spectroscopy study of PEO-based Nanocomposite polymer electrolytes. J Electrochem Soc 147(5):1718–1721
55. Aziz SB, Brza MA, Mohamed PA, Kadir MFZ, Hamsan MH, Abdulwahid RT, Woo HJ (2019) Increase of metallic silver nanoparticles in Chitosan: AgNt based polymer electrolytes incorporated with alumina filler. Results in Physics 13:102326
56. Bar N, Basak P, Tsu Y (2017) Vibrational and impedance spectroscopic analyses of semi-interpenetrating polymer networks as solid polymer electrolytes. Phys Chem Chem Phys 19:14615–14624
57. Aziz SB, Abdullah RM, Kadir MFZ, Ahmed HM (2019) Non suitability of silver ion conducting polymer electrolytes based on chitosan mediated by barium titanate ($BaTiO_3$) for electrochemical device applications. Electrochim Acta 296:494–507
58. Wieczorek W, Stevens JR (1997) Impedance spectroscopy and phase structure of polyether−poly(methyl methacrylate)−$LiCF_3SO_3$ blend-based electrolytes. J Phys Chem B 101:1529–1534
59. Aziz SB, Woo TJ, Kadir MFZ, Ahmed HM (2018) A conceptual review on polymer electrolytes and ion transport models. J Sci 3:1–17
60. Suvarna RP, Rao KR, Subbarangaiah K (2002) A simple technique for a.c. conductivity measurements. Bull Mater Sci 25:647–651
61. Venkateswarlu M, Satyanarayana N (1998) AC conductivity studies of silver based fast ion conducting glassy materials for solid state batteries. Mater Sci Eng B 54:189–195
62. Rani MSA, Ahmad A, Mohamed NS (2017) Influence of nanosized fumed silica on physicochemical and electrochemical properties of cellulose derivatives-ionic liquid biopolymer electrolytes. Ionics 24:807–814
63. Diederichsen KM, Mcshane EJ, Mccloskey BD (2017) Promising routes to a high Li+ transference number electrolyte for Lithium ion batteries. ACS Energy Lett 2:2563–2575
64. Tripathi M, Tripathi SK (2017) Electrical studies on ionic liquid-based gel polymer electrolyte for its application in EDLCs. Ionics (Kiel) 23:2735–2746
65. Samsi NS, Ali RM, Zakaria R, Yahya MZA, Ali AMM (2015) Electrical properties of ammonium iodide doped cellulose acetate based polymer electrolyte. ICGSCE 2014:331–338
66. JIBREEL UMARM, BHATTACHARYA B (2018) Synthesis, Characterization, and Detailed Studies on Plasticized Poly(ethyl methacrylate): NH4I Polymer Electrolyte. Adv Polym Technol 37:21693
67. Ali RM, Harun NI, Ali AMM, Yahyaa MZA (2012) Effect of ZnS Dispersoid in structural and electrical properties of plasticized CA-NH4I. Phys Procedia 2012(25):293–298
68. Gupta H, Shalu LB, Singh VK, Singh SK, Tripathi AK, Verma YL, Singh RK (2017) Effect of temperature on electrochemical performance of ionic liquid based polymer electrolyte with Li/LiFePO4 electrodes. Solid State Ionics 309:192–199
69. Tian Khoon L, Ataollahi N, Hassan NH, Ahmad A (2016) Studies of porous solid polymeric electrolytes based on poly (vinylidene fluoride) and poly (methyl methacrylate) grafted natural rubber for applications in electrochemical devices. J Solid State Electrochem 20(1):203–213
70. Kasprzak D, Stępniak I, Galiński M (2018) Electrodes and hydrogel electrolytes based on cellulose: fabrication and characterization as EDLC components. J Solid State Electrochem 22:3035–3047
71. Murashko K, Nevstrueva D, Pihlajamäki A, Koiranen T, Pyrhönen J (2017) Cellulose and activated carbon based flexible electrical double-layer capacitor electrode: preparation and characterization. Energy 119:435–441
72. Pérez-Madrigal MM, Edo MG, Aleman C (2016) Powering the future: application of cellulose-based materials for supercapacitors. Green Chem 18(22):5930–5956
73. Wang Z, Tammela P, Strømme M, Nyholm L (2017) Cellulose based supercapacitors: material and performance considerations. Adv Energy Mater 7:1–22
74. Varzi A, Balducci A, Passerini S (2014) Natural cellulose: a green alternative binder for high voltage electrochemical double layer capacitors containing ionic liquid-based electrolytes. J Electrochem Soc 161(3):A368–A375
75. Kasprzak D, Stępniak I, Galiński M (2018) Acetate- and lactatebased ionic liquids: synthesis, characterisation and electrochemical properties. J Mol Liq 264:233–241

76. Kant R, Singh MB (2017) Theory of the electrochemical impedance of mesostructured electrodes embedded with heterogeneous micropores. J Phys Chem C 121(13):7164–7174
77. Pohlmann S, Olyschläger T, Goodrich P, Vicente JA, Jacquemin J (2015) Balducci a mixtures of Azepanium based ionic liquids and propylene carbonate as high voltage electrolytes for supercapacitors. Electrochim Acta 153:426–432
78. Acharya S, Hu Y, Moussa H, Abidi N (2017) Preparation and characterization of transparent cellulose films using an improved cellulose dissolution process. J Appl Polym Sci 134:1–12
79. Ajina A, Isa D (2010) Symmetrical Supercapacitor using coconut Shell-based activated carbon. Pertanika J Sci & Technol 18(2):351–363
80. Yusof YM. Characteristics of corn starch/chitosan blend green polymer electrolytes complexed with ammonium iodide and its application in energy devices. University of Malaya 2017, Malaysia, Dissertation
81. Shukur MF. Characterization of ion conducting solid biopolymer electrolytes based on starch-chitosan blend and application in electrochemical devices. University of Malaya 2015, Malaysia, Dissertation
82. Majid, S.R. High molecular weight chitosan as polymer electrolyte for electrochemical devices. Doctoral thesis, University of Malaya 2007, Kuala Lumpur, Malaysia
83. Liew C-W, Ramesh S, Arof AK (2015) Characterization of ionic liquid added poly(vinyl alcohol)-based proton conducting polymer electrolytes and electrochemical studies on the supercapacitors. Int J Hydrog Energy 40:852–862
84. Shuhaimi NEA, Teo LP, Woo HJ, Majid SR, Arof AK (2012) Electrical double-layer capacitors with plasticized polymer electrolyte based on methyl cellulose. Polym Bull 69:807–826
85. Pandey G, Kumar Y, Hashmi S (2011) Ionic liquid incorporated PEO based polymer electrolyte for electrical double layer capacitors: a comparative study with lithium and magnesium systems. Solid State Ionics 190(1):93–98
86. Kamarudin KH, Hassan M, Isa MIN (2018) Lightweight and flexible solid-state EDLC based on optimized CMC-NH_4NO_3 solid bio-polymer electrolyte. ASM Sci J 11(1):29–36